Observation and origin of an interannual salinity anomaly in the Mozambique Channel

P. M. van der Werf,[1] M. W. Schouten,[2] P. J. van Leeuwen,[1] H. Ridderinkhof,[2] and W. P. M. de Ruijter[1]

[1] A positive salinity anomaly of 0.2 PSU was observed between 50 and 200 m over the years 2000–2001 across the Mozambique Channel at a section at 17°S which was repeated in 2003, 2005, 2006, and 2008. Meanwhile, a moored array is continued from 2003 to 2008. This anomaly was most distinct showing an interannual but nonseasonal variation. The possible origin of the anomaly is investigated using output from three ocean general circulation models (Estimating the Circulation and Climate of the Ocean, Ocean Circulation and Climate Advanced Modeling, and Parallel Ocean Program). The most probable mechanism for the salinity anomaly is the anomalous inflow of subtropical waters caused by a weakening of the northern part of the South Equatorial Current by weaker trade winds. This mechanism was found in all three numerical models. In addition, the numerical models indicate a possible salinization of one of the source water masses to the Mozambique Channel as an additional cause of the anomaly. The anomaly propagated southward into the Agulhas Current and northward along the African coast.

1. Introduction

[2] The circulation around Madagascar is characterized by its high variability [*DiMarco et al.*, 2002; *Quartly and Srokosz*, 2004; *de Ruijter et al.*, 2005; *Hermes et al.*, 2007]. The main inflow into this area is from the South Equatorial Current (SEC), which impinges on the island from the east between 10°–20°S (Figure 1). There, it bifurcates into a northward and southward branch, being the Northeast and Southeast Madagascar Currents (NEMC and SEMC), respectively. The northward branch follows the northeast coast of the island and flows westward toward the African coast, where it bifurcates once more. Part of the flow of the SEC thus enters the Mozambique Channel. Observations have shown that the flow in the Mozambique Channel consists of a train of eddies, rather than a continuous current [*de Ruijter et al.*, 2002; *Ridderinkhof and de Ruijter*, 2003]. In the southern part of the channel, the eddies from the Mozambique Channel meet with the highly variable flow from the Southeast Madagascar Current, and move into the Agulhas Current. *Schouten et al.* [2002] have shown that the variability around Madagascar controls the shedding rate of Agulhas Rings. The latter feed into the overturning circulation of the Atlantic Ocean [*de Ruijter et al.*, 1999; *Gordon*, 1986; *Biastoch et al.*, 2008].

[3] To study the variability in the Mozambique Channel, an array of moored current and conductivity-temperature-depth (CTD) meters has been placed in the channel at 17°S as part of the Dutch Long-term Climate Observations (LOCO) program. Since 2003, CTD meters have been placed in the upper part of one of the moorings (Figure 2). Moreover, six hydrographic sections have been taken at this location in the period 2000 to 2008.

[4] A positive salinity anomaly is observed in the upper layers of the Mozambique Channel in the years 2000 and 2001. In this paper we will present and discuss the observations of this anomaly and its possible origin.

[5] The waters in the Mozambique Channel consist of a mixture of different water masses. The observed anomaly in the salinity content of the mixture could be caused by either an increased salinity of one of the source waters, or a change in the mixing ratio of these source waters. The main source waters in the upper layers are the Subtropical Surface Water (STSW), the Tropical Surface Water (TSW), and the Indonesian Throughflow Water (ITFW).

[6] The STSW is formed by strong evaporation between 25°–35°S, and subducts below the fresher waters in the north [*Wyrtki*, 1973; *Karstensen and Quadfasel*, 2002]. The salinity maximum erodes northward, but remains clearly distinguishable owing to southward Ekman transport of fresher tropical waters in the upper layer [*Song et al.*, 2004]. Each austral summer, an eddy of STSW is formed in the Mozambique Channel [*Schouten et al.*, 2005].

[7] The ITFW signal is found along a zonal band across the basin (10°–15°S) [*Wyrtki*, 1971; *Gordon*, 1986]. The deeper component of the throughflow has also been traced along a zonal trajectory across the basin [*Talley and*

---

[1]Institute for Marine and Atmospheric Research Utrecht, Utrecht University, Utrecht, Netherlands.
[2]Department of Physical Oceanography, Royal Netherlands Institute for Sea Research, Texel, Netherlands.
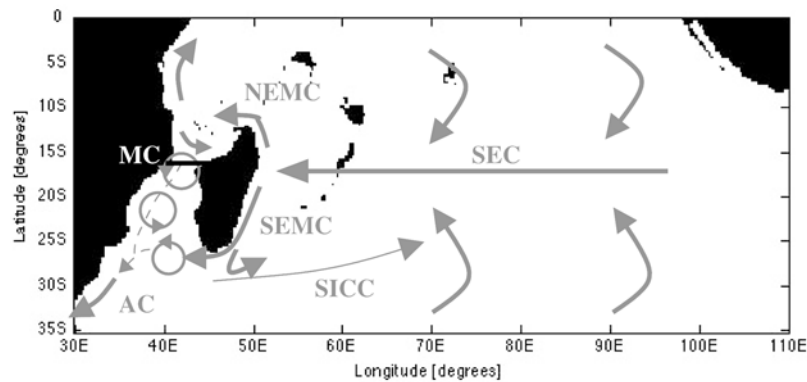
Figure 1. Sketch of the South Indian Ocean at 250 m depth with the main currents (gray) and the measurement section in the Mozambique Channel (MC), which stretches from 40°–42.4°E at 17°S (black). The main currents are South Equatorial Current (SEC), Southeast Madagascar Current (SEMC), Northeast Madagascar Current (NEMC), South Indian Ocean Countercurrent (SICC), and the Agulhas Current (AC).

Sprintall, 2005], but has not been identified west of the Mascarene ridge around 60°E. Nonetheless, the characteristics of the ITFW have their imprint on the water mass characteristics all over the South Indian Ocean thermocline [*You and Tomczak*, 1993; *You*, 1997].

[8] In the recent past, several studies were concerned with salinity variations of water masses in the Indian Ocean. *Bryden et al.* [2003] and *McDonagh et al.* [2005] report on a freshening of the upper thermocline along 32°S before 1987 and a salinization afterward. During El Niño (La Niña), the precipitation above the Indonesian Seas is below (above) average, causing a salinization (freshening) of the ITFW [*Phillips et al.*, 2005]. *Nauw et al.* [2006] observed two anomalously salty intrathermocline eddies in the boundary current southeast of Madagascar, that originated from the southeast Indian Ocean.

[9] A change in mixing ratios of the source waters can be caused by wind variations. A prominent example is the latitudinal variation of the SEC caused by the Indian Ocean Dipole (IOD) [*Palastanga et al.*, 2006]. During an IOD+, the SEC is shifted to the north and more relatively saline water from the subtropical gyre can enter the Mozambique Channel. On the other hand, during an IOD−, the SEC is shifted to the south and more relatively fresh water (TSW and ITFW) can enter the channel.

[10] Mixing ratios can also change further upstream. For example, the transport of the Indonesian Throughflow is reduced during El Niño's [*Gordon et al.*, 1999; *Phillips et al.*, 2005; *Susanto et al.*, 2001; *Vranes et al.*, 2002].

[11] The aim of the present paper is to describe the observed anomaly and determine its origin. In section 2 the observations of the salinity anomaly in the Mozambique Channel are described. The observational data show that the anomaly is an interannual phenomenon that is not caused by local forcing. Because of a lack in temporal and spatial resolution of measurements in the Indian Ocean, we have to make use of numerical models to determine the origin. These models are the Estimating the Circulation and Climate of the Ocean (ECCO) model, the Ocean Circulation and Climate Advanced Modeling (OCCAM) model, and the Parallel Ocean Program (POP) model. These three models were chosen because their salinity fields in the Mozambique

Channel were similar to the observations and their data spanned a sufficiently long period. In section 3, the models are introduced and their salinity time series in the Mozambique Channel are studied. Then, the sources and path of the anomaly will be studied using the numerical models in section 4. We will conclude with a summary and discussion of our main results.

2. Observations

[12] Measurements of salinity, temperature, and velocities at different depths in the Mozambique Channel have been carried out both by a moored array and by a hydrographic section, which was repeated six times at the location of the moored array. This moored array is placed across the Mozambique Channel at its narrowest section around 17°S (Figure 1).
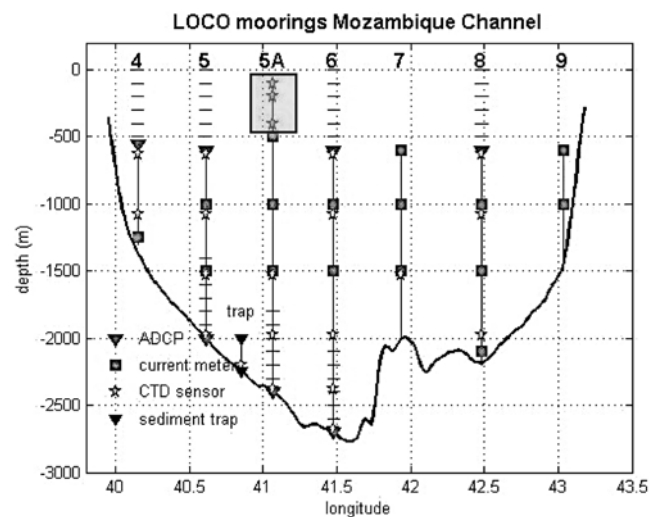

Figure 2. Mooring configuration in the Dutch Long-term Climate Observations program (November 2003 to January 2008). Mooring 5A has been fitted with three conductivity-temperature-depth (CTD) meters in the top 500 m (gray box).
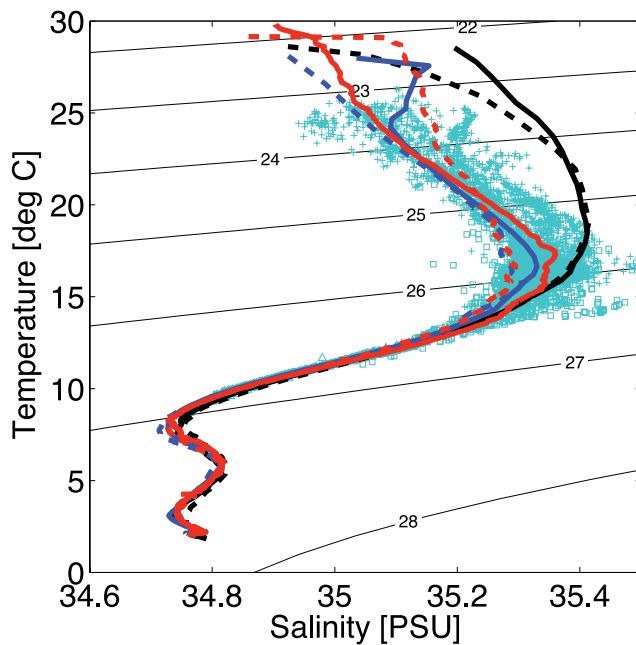
Figure 3. Six section-averaged temperature-salinity (T-S) curves of the years 2000 (solid black), 2001 (dashed black), 2003 (solid blue), 2005 (dashed blue), 2006 (solid red), and 2008 (dashed red line) overlaying daily averages of T-S measured continuously at mooring 5A (Figure 2) between November 2003 and January 2008 (cyan markers) by CTD sensors at 100 m (plusses), 200 m (squares), and 400 m (triangles).

[13] During deployment and recovery of the mooring array, six hydrographic sections over the full width of the channel were made. In the years 2000 and 2001, the section was sampled in March and April from aboard RV Pelagia, whereas in 2003 the moorings were serviced in November utilizing the RRS Charles Darwin. In February and March 2005 and in March and April 2006 the section was revisited by RRS Discovery. The last sampling of the section was in January and February 2008 by the RV Meteor.

[14] In the period between the 2003 and 2008 occupations of the section, continuous observations of temperature and salinity were made by 22 Seabird 37-SM CTD sensors attached to the moorings (Figure 2). These observations allow us to assess the water mass characteristic variability on shorter time scales than allowed for by the hydrographic sections, and to verify how much of the observed interannual differences should be attributed to shorter time scales, e.g., those associated with the passage and formation of Mozambique Channel eddies.

[15] Three CTD sensors were located in the upper layers, at nominal depths of 100, 200, and 400 m in the top part of mooring 5A located in the central part of the channel near 41.1°E. Vertical motion of the moored instruments is considerable (downward excursions up to 100 m are recorded) owing to the strong currents in the channel. Combined with the vertical motion of the isopycnals associated with the passage of Mozambique eddies, the three sensors cover most of the upper 400 m density range.

[16] Results of the six occupations and the moored array are summarized in Figure 3. Large differences in T/S

characteristics between the six occupations of the section (lines) are readily observed. Averaged on levels of potential density (σ_0) the first 2 years (2000 and 2001) are more saline than the last 4 years by over 0.2 PSU in the upper 200 m. Except for the very fresh waters found in 2001 in the uppermost 50 m, the first two profiles (2000 and 2001) are very similar. Their maximum salinity is situated at 130 m depth. Between 100 and 200 m, the 2003, 2006, and 2008 thermoclines were significantly warmer and fresher, with a sharp salinity maximum at 200 m depth. In 2005, a similarly fresh thermocline is observed, with a salinity maximum at 170 m depth.

[17] The anomaly is maximal around the $\sigma_o = 24.5$ level, which has a climatological depth between 125 m and 150 m (Figure 4b). The anomaly is therefore well covered by the continuous CTD measurements at the moorings within the period November 2003 to January 2008. The moored measurements are spaced around the last four hydrographic measurements (2003–2008; Figure 3), and are overall much fresher than the first two hydrographic measurements. The fresher branch is climatologically more 'normal' (Figure 4). We cannot completely rule out the possibility that the two more saline sections (2000 and 2001) were unrepresentative of the period in between these sections, but it is clear from the continuous observations over 2003–2008 that the 2000 and 2001 sections were anomalously saline with respect to the complete period 2003–2008. This indicates that the measurement of the high salinity in 2000 and 2001 was not the product of the sampling in different seasons. Moreover, the hydrographic section taken in 2006 took place in the same season as those taken in 2000 and 2001.

[18] This is quite a surprising result because of the strong seasonality in regions close to Madagascar due to the monsoon variation. However, even in individual CTD recordings at the moorings, there was no seasonal cycle observed.

[19] The anomaly was also not caused by local rainfall. Although the net precipitation in 2000 was anomalously low, in the austral summer of 2001 the rainfall in the northern part of the Mozambique Channel was anomalously high. This resulted in the very fresh waters in the uppermost 50 m of 2001, but had no influence on the salinity at the depth of the anomaly, which is below the mixed layer.

[20] In addition, no correlation has been found between the 2000–2001 salinity anomaly and the local background flow. An anticyclonic Mozambique Channel eddy was observed during the survey of 2000, while in 2001 a cyclonic anomaly was present. In summary, we conclude that the anomaly is an interannual phenomenon that originated upstream in the Indian Ocean.

[21] Inspection of the annual mean salinity distributions from the World Ocean Atlas 2001 [Conkright et al., 2002] gives a clue about the background of the observed differences. In particular, we are interested in the isopycnal surface at $\sigma_o = 24.5$, where the largest salinity difference between the 2000 and 2001 hydrographic sections and the 2003–2008 period is observed (Figure 4). The observed salinities at that isopycnal level over the 4-year continuous observational period ($S \approx 35.2$ PSU) are close to climatological values for the SEC region near the northern tip of Madagascar from where most of the water entering the Mozambique Channel is likely derived. The years 2000
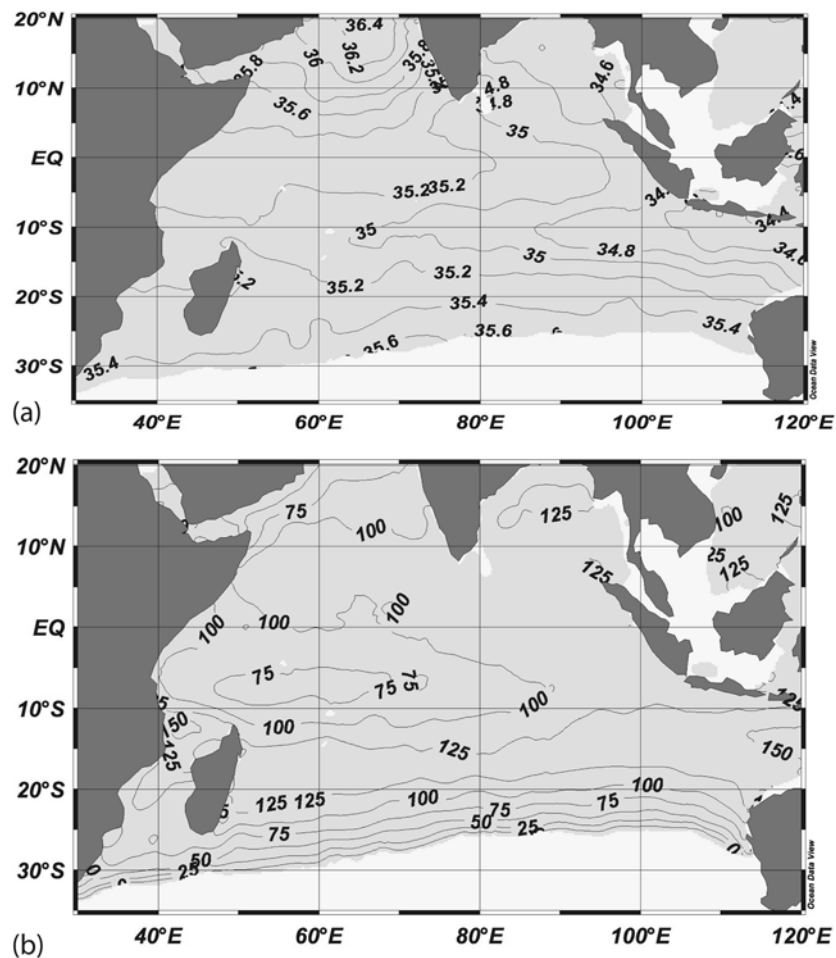
Figure 4. (a) Salinity at the 24.5 isopycnal layer. (b) Depth of this isopycnal layer. Annual mean climatological data were extracted from the World Ocean Atlas 2001 [*Conkright et al.*, 2002].

and 2001 appear anomalously saline, with salinities corresponding to those found in the subtropical gyre further south ($S \approx 35.4$ PSU; Figure 4a). An explanation for the anomalously high salinities in the upper thermocline of the Mozambique Channel may therefore be found in anomalously large inflow of subtropical water from that source.

3. Analysis of the Anomaly in Numerical Models

[22] Since there is not enough observational data, we have studied the output of three ocean general circulation models: the Estimating the Circulation and Climate of the Ocean (ECCO) model, the Ocean Circulation and Climate Advanced Modeling (OCCAM) model, and the Parallel Ocean Program (POP) model.

[23] The ECCO configuration used is the one used for a quasi-operational analysis [*Menemenlis et al.*, 2005]. The model is based on the MITgcm [*Marshall et al.*, 1997]. Its output is available on http://ecco.jpl.nasa.gov/, of which we studied the data set with Kalman Filter assimilation. Our data set starts in 1993 and ends in 2005 with a 10-day output interval. The data set has a zonal grid spacing of $1°$ and a meridional grid spacing increasing from $1/3°$ within $10°$ of the equator to $1°$ poleward of $22°$N/S. This coarse resolution implies that the observation section at $17°$S is

represented by only 5 grid cells in the horizontal. There are 46 levels in the vertical direction, with a vertical resolution of 10 m in the top 150 m. Atmospheric forcing was applied by 12-hourly wind stress and daily heat and freshwater fluxes from NCEP. (More information about this model run and the assimilation can be found in the work by *Menemenlis et al.* [2005].)

[24] The OCCAM model [*Webb et al.*, 1998; *Coward and de Cuevas*, 2005] was derived from the Bryan-Cox-Semtner general ocean circulation model. In this study, we analyzed the output of model run 103 (available at http://www.noc.-soton.ac.uk/JRD/OCCAM/EMODS/select.php), spanning the period 1989 to 2005. It has a 5-day mean output, a horizontal resolution of $1/4°$ and 66 layers in the vertical direction, with 14 layers in the top 100 m. Since the run was started from 1985 from Levitus temperature and salinity and zero velocity and thus had a shortened spin-up (B. A. de Cuevas, personal communication, 2007), the first years of the output (1989–1992) could not be used for analysis. Therefore, our data set stretches from January 1993 to December 2004. Atmospheric forcing was applied by NCEP 6-hourly forcing [*Coward and de Cuevas*, 2005].

[25] The POP model [*Dukowicz and Smith*, 1994] was also derived from the Bryan-Cox-Semtner code. The model has a $1/10°$ horizontal resolution and 40 layers in the
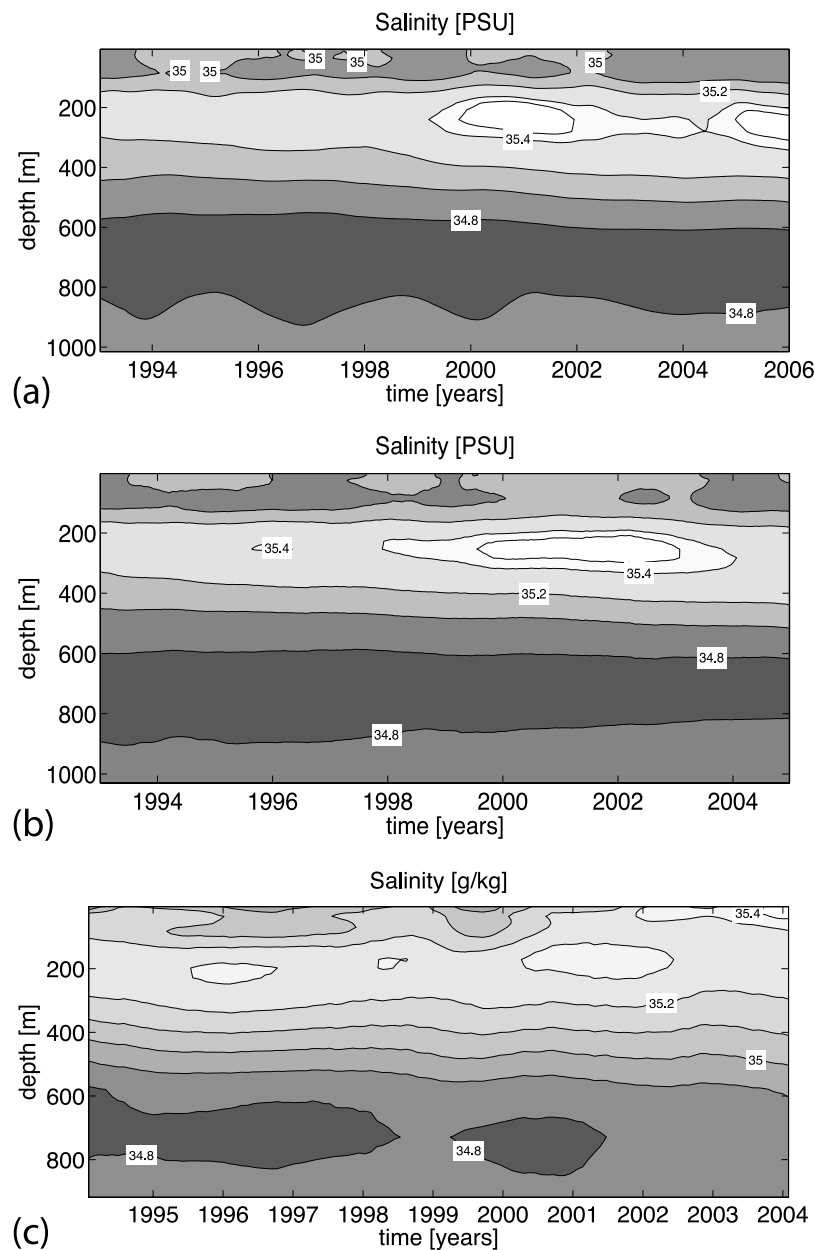
Figure 5. Section-averaged salinity at 17°S in the Mozambique Channel (Figure 1) in (a) ECCO, (b) OCCAM, and (c) POP. Contours are drawn every 0.2 PSU and at 35.45 PSU for ECCO and OCCAM and every 0.1 g/kg for POP. In ECCO, a salinity anomaly is seen in the layer of maximum salinity (around 240 m depth) from the end of 1999 to the end of 2001. A second anomaly starts around the same depth in 2005. In OCCAM, a salinity anomaly is seen in the layer of maximum salinity (around 253 m depth) from 2000 to the end of 2002. In POP, three salinity anomalies are seen in the layer of maximum salinity. The anomaly that stretches from 2000 to March 2002 has its core at 171 m depth.

vertical, with 9 in the top 100 m. The data set stretches from 1994 to the end of 2003 and has a monthly mean output. Also for this run, the atmospheric forcing was applied by NCEP (daily). A more detailed description of this model run can be found in the work by *Maltrud and McClean* [2005].

[26] The area studied in all the models stretches from 30°–110°E and from the equator to 35°S. Most of the analysis was performed in the top 1000 m. Since the salinity anomaly in the observations was shown to be an interannual phenomenon (section 2), we have conducted all analysis of the numerical models after yearly smoothing of the data sets, which emphasizes the interannual variations.

[27] Section-averaged salinity time series from the numerical models at the section in the Mozambique Channel (17°S; Figure 1), show qualitatively similar results to the observations. All three models show an anomaly around the years 2000 and 2001 (Figure 5). The amplitude of these anomalies is a bit smaller than in the observations, in the order of 0.1 PSU. This is partly due to the high diffusivity in the models and to the time smoothing of the signals. The
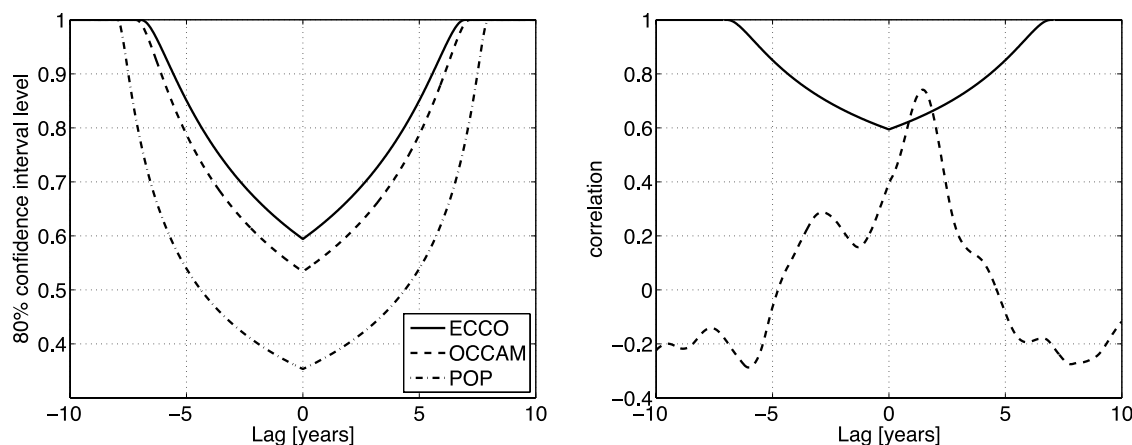
Figure 6. (left) The 80% confidence levels for the three models as a function of the lag in a correlation. Correlations smaller than these confidence levels are considered insignificant and are not taken into account in further analysis. (right) Example of the correlation function between the salinity time series at 12°S, 70°E and the reference time series in ECCO (dashed line). The correlation is only significant when the correlation exceeds the 80% confidence level (solid line), which is for lags between 0.8 and 1.8 years in this example.

depth of the anomalies in the three models is respectively 240 m, 253 m, and 171 m for ECCO, OCCAM, and POP, which are all in the layer of maximum salinity. The anomalies in the models are thus a bit deeper than in the observations. However, the anomalies in the observations and in the models are all situated well below the mixed layer. As in the observations, the anomalies in the numerical models are interannual phenomena. Their origin may therefore be found in interannual, large-scale variations in the Indian Ocean. In view of the similarities between the observations and the models, and despite the somewhat deeper level of the anomalies in the models, we assume the anomalies in the models of similar nature as the anomalies in the observations.

4. Path of the Anomalies in the Models

[28] The source areas of the anomaly were found by a method based on correlation functions, which is explained below by using the results from ECCO. First, the ECCO-simulated data of layer 20 (240 m depth) from the section-averaged salinity time series across the Mozambique Channel (described above) is selected as reference time series. This layer was chosen because it intersects the center of the anomaly.

[29] This salinity time series is then correlated to the time series of several variables at all the grid points of the domain. Our focus has been on the salinity and zonal and meridional velocity time series. A positive correlation with the salinity time series indicates that the increase of salinity of one of the source waters could be the origin of the salinity anomaly in the Mozambique Channel. On the other hand, a correlation with the velocity time series indicates a changing transport of source waters. First, we will analyze the salinity field in ECCO.

[30] At each point in the domain, a correlation function is derived. Only those parts of the correlation functions that have coefficients higher than the 80% confidence interval level are included in the analysis. This significance level has

been calculated following *Bendat and Piersol* [1986]. We have computed the number of independent variables as the ratio of the total number of data points in the time series to the number of points between zero and the first $1/e$ crossing of the autocorrelation function of the reference time series. Figure 6 shows the significance level as a function of the lag for each of the models. For zero lag, the significance level is 0.59, 0.53 and 0.35 for ECCO, OCCAM, and POP, respectively. At longer lags, the number of points decreases and therefore the significance level increases exponentially (Figure 6). In ECCO, when using this constraint at lags of 5 years, the correlation coefficient should be larger than 0.85 to be significant, while for lags larger than 7 years coefficients are never significant. As a result, we are not able to trace the anomalies back for more than 5 years in practice.

[31] Finally, the results of all grid points are combined to obtain an overview at the basin scale. All layers are analyzed equally. However, our results can be summarized by the layer of the reference time series (Figures 7a and 7b). In Figure 7a, the maximum significant correlation coefficient at each point is shown; the lags corresponding to these maxima are displayed in Figure 7b. Positive lags indicate that the correlated anomaly at the particular grid cell occurred before the anomaly in the mooring section; negative lags indicate that the correlated anomaly occurred after the anomaly in the section. Anomalies propagate from grid cells with large positive lags, via areas with zero lag, toward the cells with large negative lags. Along their paths, the anomalies remain in a positive correlation with the anomaly at the reference section. A pathway of an anomaly should be continuous in time, i.e., jumps in the lag are unphysical. These unphysical paths shall not be considered in the analysis.

[32] As expected, the correlation of the averaged section in the Mozambique Channel with a point at that section is almost one and has a zero lag. Upstream (downstream) the lag increases (decreases). The largest lag in a direct physical path with the mooring section can be seen at 85.5°E,
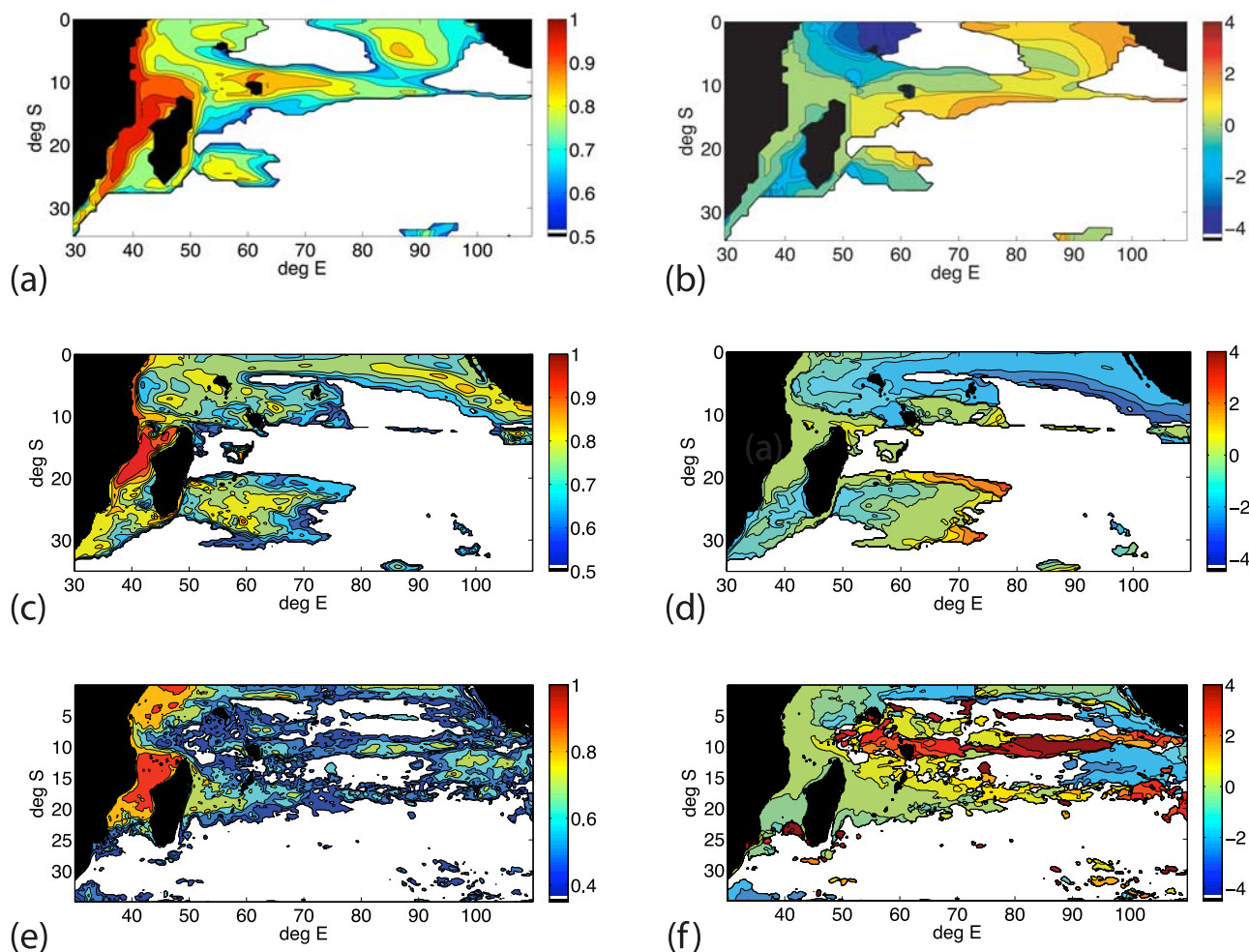
Figure 7. Values of (left) maximum correlation and (right) lags corresponding to these maxima (in years) for correlations of the salinity time series at each point in the domain with the section-averaged salinity time series in the Mozambique Channel at the depth of the salinity anomaly. Only significant correlations are displayed (see section 4). (a and b) ECCO (240 m depth), (c and d) OCCAM (253 m depth), (e and f) POP (171 m depth). Positive lags denote that the anomaly at that point appeared before the anomaly in the Mozambique Channel.

12.5°S, and is 2 years (Figure 7b). Its correlation coefficient is 0.74, which is slightly larger than the significance level at this lag. From there, the anomaly moves westward in the SEC toward Madagascar. The vertical extent of this path is roughly from 150 m to 330 m depth. At the African coast, one part moves southward into the Mozambique Channel and the Agulhas Current. An other part moves north along the African coast. This latter part is also fed by another path extending directly from the eastern boundary of the domain. Note that the anomaly could not travel from 85.5°E northward, since there is a jump in lags at 11°S. In the northern part of the domain, around 60°E, 5°S, the signal is correlated with a negative lag up to the surface, which is probably due to wind forced upwelling.

[33] To verify whether the transported signal is the salinity anomaly itself, we studied the salinity time series in a 2° × 2° region around 85.5°E, 12.5°S (Figure 9a). Indeed, a salinity anomaly is present at this location 2 years before it is observed in the Mozambique Channel. The anomaly stretches from 75 to 280 m depth and has its maximum in June 1998. The amplitude of the simulated

anomaly is only 0.07 PSU, which makes it improbable that this anomaly is the only cause of the anomaly in the Mozambique Channel.

[34] The change in lag along the path is directly related to the background velocity along the streamlines of the path. Extrapolating the path backward in time, the anomaly originates from the Indonesian waters at the end of 1997. The occurrence of both an El Niño and a positive IOD explains the salinity increase of this water.

[35] The correlation analysis method conducted on the zonal and meridional velocity fields yields a second origin in ECCO for the salinity anomaly. In Figures 8a and 8b, a positive correlation to the zonal velocity with an area stretching around 86.5°E, 14°S is observed. A positive correlation in a westward flowing current (SEC; zonal velocity is defined positive eastward) means a weakening of that current. Note that the correlation is primarily found at the northern limit of the SEC, which means that the speed of especially the TSW and ITFW is weakened. The lag of this region with the Mozambique Channel is 9 months. Figure 9b shows that the anomaly is 3 cm/s, and that it
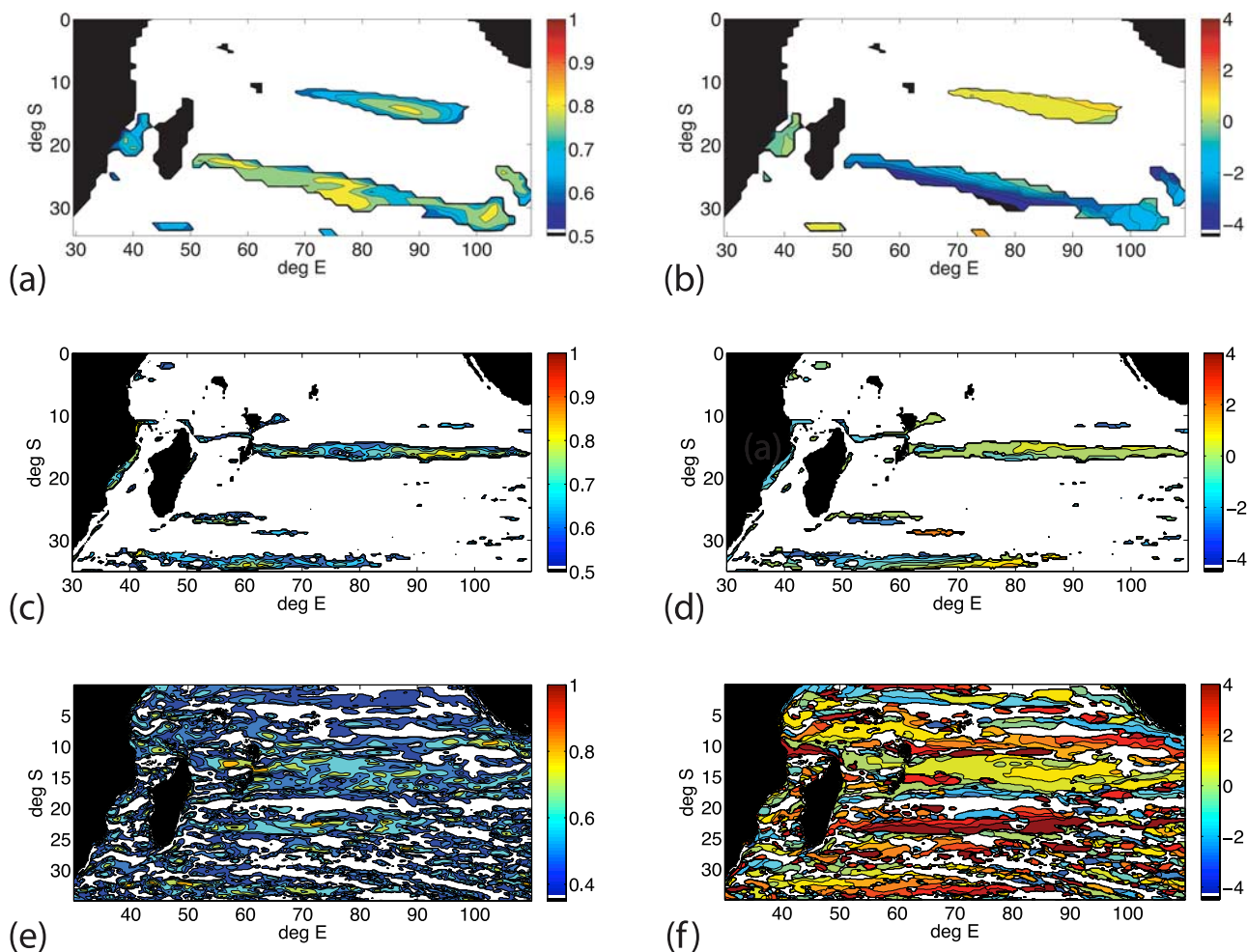
Figure 8. As Figure 7 but now for correlations with the zonal velocity time series at each point (positive eastward).

reaches to the surface. An estimation of the salinity increase caused by this velocity anomaly of fresh waters, taken into account its width and hight, is in the order of 0.1 PSU.

[36] *Lee* [2004] and *Lee and McPhaden* [2008] have shown that the zonal wind stress south of the Equator (20°–0°S) weakened over the period 1992–2000 and increased afterward. The transport variation estimated by *Lee* [2004] from the amplitude of this wind stress variation and Sverdrup theory is in agreement with the transport variation we have found.

[37] A second region of positively correlated zonal velocity in ECCO is apparent in Figures 8a and 8b. However, this region has a negative lag and can therefore not be the cause of the salinity anomaly in the Mozambique Channel.

[38] Results from the model OCCAM differ from the above findings for the salinity field correlations, but are quite similar for the velocity field correlations. Figures 7c and 7d show a connection to the subtropical gyre, but not to the Indonesian Throughflow. The first point of the path is found at 77.5°E, 21°S and has a lag of 2.8 years. The anomaly at this point has an amplitude of 0.1 PSU (Figure 9c). It follows the northern border of the band, with a velocity in agreement with the streamlines. The correlated region

stretches from 205 m to 609 m depth. Then, the signal travels via the NEMC in a very narrow band along the coast, which is more apparent in the lower layers. As in the results of ECCO, the signal splits at the African coast, partly northward along the coast and partly through the Mozambique Channel into the Agulhas Current.

[39] There is no direct physical explanation to the origin of this particular anomaly. However, when applying the correlation function method without significance constraints, the anomaly could be traced further back in time, to a region around 95°E and 27°S where it appeared in 1993 as an area of high salinity. Although its origin is undeterminable in the model output, the salinity anomaly is comparable to the observations of *Bryden et al.* [2003] and *McDonagh et al.* [2005], who found an increase in salinity in the thermocline east of 80°E along 32° in 1995 relative to 1987, and a decrease between 1995 and 2002.

[40] As in ECCO, the anomaly in OCCAM has a positive correlation with the zonal velocity of the SEC (Figures 8c and 8d). The amplitude of the anomaly is 5 cm/s (Figure 9d), slightly higher than in ECCO. However, since the width of the region is smaller in OCCAM, this again results in a
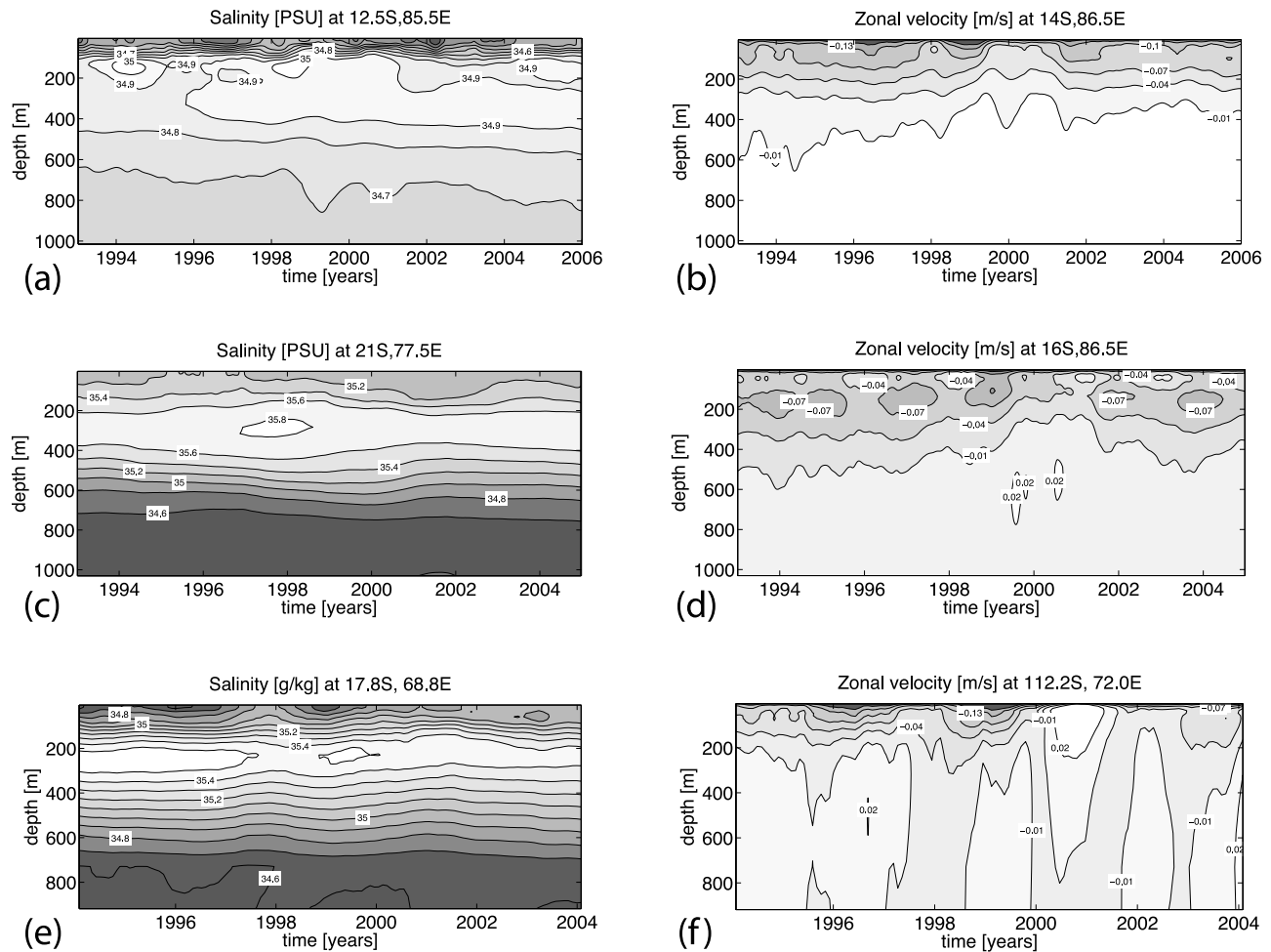
Figure 9. (left) Anomalies in salinity at the starting point of the path physically realistically leading to the Mozambique Channel. (right) Anomalies in zonal velocity at the core of the highly correlated region. (a and b) ECCO, (c and d) OCCAM, (e and f) POP. The time series have been averaged over a $2° \times 2°$ region around the location defined in the title of each plot.

salinity anomaly in the Mozambique Channel in the order of 0.1 PSU.

[41] The results of POP are harder to interpret, since the reference time series shows three anomalies, all 2 years from each other. The highest correlations will therefore be given to time series that correlate with all three anomalies. However, the significance levels are much lower because of this, and Figures 7e and 7f and 8e and 8f show a lot of regions that are not cause-effect related to the salinity anomaly of 2000–2001. For the analysis of POP we will therefore focus even more on the highest correlations with physically realistic paths.

[42] Only the salinity fields above 200 m depth are correlated to the Mozambique Channel anomaly. As in ECCO, the anomaly originates from the SEC (Figures 7e and 7f), but it is not connected to the Indonesian Through-flow, rather to the subtropical part of the SEC, as can be seen from the high background salinity found around the first point of the path (68.8°E, 17.8°S, with a lag of 8 months; Figure 9e). In contrast to ECCO and OCCAM, the salinity anomaly in POP emerged in the model's time

and spatial domain. In Figure 9e, we see that it is not the anomaly in the maximum salinity layer that correlates with a lag of 8 months, but the upwelling of isohalines instead. This upwelling is caused by an anomalous negative wind curl of 0.01 N/m. Note that the maximum salinity layer is deeper than 200 m, where no correlation path has been found.

[43] In the results for the correlation of the zonal velocity field there is a lot of noise. However, as in the results for ECCO and OCCAM, the SEC is weakening at its northern limit just before the salinity anomaly in the Mozambique Channel (lag is 10 months).

[44] To summarize the above results, we have found a salinity anomaly in all three numerical models that resembles the anomaly as observed in the LOCO project. The three models do not give us a unique cause for the origin of the anomaly in the salinity field. Nonetheless, all three models show a correlation with the strength of the SEC, which is related to a decrease in the wind stress [*Lee*, 2004; *Lee and McPhaden*, 2008], and the advection of a salinity anomaly formed elsewhere in the basin. Given the agree-

ment in the models on the weakening of the SEC, we conclude that this mechanism is likely a major part of the origin of the anomaly found in the observations.

5. Conclusions and Discussion

[45] The aim of this study was to describe and explain the variations in the salinity field observed in the Mozambique Channel. In 2000 and 2001, we have found a strong positive salinity anomaly both in in situ measurements and in three numerical models (ECCO, OCCAM, and POP). In all cases, the anomaly was an interannual variation and not a seasonal phenomenon. The most probable origin of this anomaly is the anomalous inflow of subtropical waters caused by a weakening of the northern part of the SEC by weaker trade winds. In addition, the models indicated a possible salinization of one of the source water masses, i.e., a saltier ITFW from the 1997 El Niño and IOD+ (ECCO), a saltier patch in the southeastern Indian Ocean (already present at the start of the time series in OCCAM), or upwelling of the salinity maximum layer by a local wind curl (POP).

[46] The method we used to obtain these results was based on correlation functions. This method was less effective in the case of POP. The POP salinity time series showed three anomalies, which were regularly spaced in time. The method could not distinct correlations with the 2000–2001 anomaly from correlations with the other anomalies. This resulted in many regions which were correlated to the anomaly, but not all of which could be physically related to the 2000–2001 anomaly. This is unfortunate, since the POP run had the highest horizontal resolution of the three numerical models.

[47] In a recent paper, *Nauw et al.* [2008, Figure 6c] describe a similar salinity variation in the SEMC. In four sections around the south coast of Madagascar, the along-current salinity differences were small, of the order of 0.1 PSU or less. However, compared to data collected during a World Ocean Circulation Experiment (WOCE) survey in 1995, the salinity maximum during the occupation of 2001 was 0.2 PSU higher.

[48] In the results from the models ECCO and OCCAM, a positive correlation at zero lag of the salinity anomaly at the section in the Mozambique Channel with the sections south of Madagascar is found (Figures 7a–7d). In OCCAM the path toward the SEMC is a side branch of the path described in section 4, which means that the anomalies in the Mozambique Channel and the SEMC have a common source. There are two paths leading toward the SEMC in ECCO, one starting at the same location as the path toward the Mozambique Channel, i.e., 85.5°E, 12.5°S, and the second starting at a more southerly origin. These two origins have a common source by an insignificantly correlated path. As in the Mozambique Channel, the anomalies in the SEMC of the two numerical models have a smaller amplitude than in the in situ observations because of smoothing. This additional agreement with observations gives extra support to the results from ECCO and OCCAM, which suggested that the strength of the SEC is a major part of the origin of the anomaly found in the observations.

References

Bendat, J. S., and A. G. Piersol (1986), *Random Data, Analysis and Measurement Procedures*, 2nd ed., John Wiley, New York.

Biastoch, A., C. W. Boening, and J. R. E. Lutjeharms (2008), Agulhas leakage dynamics affects decadal variability in Atlantic overturning circulation, *Nature*, *456*, 489–492.

Bryden, H. L., E. L. McDonagh, and B. A. King (2003), Changes in ocean water mass properties: Oscillations or trends, *Science*, *300*, 2086–2088.

Conkright, M. E., H. E. Garcia, T. D. O'Brien, R. A. Locarnini, T. P. Boyer, C. Stephens, and J. I. Antonov (2002), World Ocean Atlas 2001: Objective Analyses, Data Statistics and Figures, CD-ROM Documentation, ftp://ftp.nodc.noaa.gov/pub/data.nodc/woa/PUBLICATIONS/readme.pdf, Natl. Oceanogr. Data Cent., Silver Spring, Md.

Coward, A. C., and B. A. de Cuevas (2005), The OCCAM 66 level model: Physics, initial conditions and external forcing, *Tech. Rep. 99*, Southampton Oceanogr. Cent., Southampton, U. K.

de Ruijter, W. P. M., A. Biastoch, S. S. Drijfhout, J. R. E. Lutjeharms, R. P. Matano, T. Pichevin, P. J. van Leeuwen, and W. Weijer (1999), Indian-Atlantic interocean exchange: Dynamics, estimation and impact, *J. Geophys. Res.*, *104*(C9), 20,885–20,910.

de Ruijter, W. P. M., H. Ridderinkhof, J. R. E. Lutjeharms, M. W. Schouten, and C. Veth (2002), Observations of the flow in the Mozambique Channel, *Geophys. Res. Lett.*, *29*(10), 1502, doi:10.1029/2001GL013714.

de Ruijter, W. P. M., H. Ridderinkhof, and M. W. Schouten (2005), Variability of the southwest Indian Ocean, *Philos. Trans. R. Soc., Ser. A*, *363*, 63–76.

DiMarco, S. F., P. Chapman, W. D. Nowlin Jr., P. Hacker, K. Donohue, M. Luther, G. C. Johnson, and J. Toole (2002), Volume transport and property distributions of the Mozambique Channel, *Deep Sea Res., Part II*, *49*, 1481–1511.

Dukowicz, J. K., and R. D. Smith (1994), Implicit free-surface method for the Bryan-Cox-Semtner ocean model, *J. Geophys. Res.*, *99*(C4), 7991–8014.

Gordon, A. L. (1986), Interocean exchange of thermocline water, *J. Geophys. Res.*, *91*(C4), 5037–5046.

Gordon, A. L., R. D. Susanto, and A. Ffield (1999), Throughflow within Makassar Strait, *Geophys. Res. Lett.*, *26*(21), 3325–3328.

Hermes, J. C., C. J. C. Reason, and J. R. E. Lutjeharms (2007), Modeling the variability of the greater Agulhas Current system, *J. Clim.*, *20*, 3131–3146, doi:10.1175/JCLI4154.1.

Karstensen, J., and D. Quadfasel (2002), Water subducted into the Indian Ocean subtropical gyre, *Deep Sea Res., Part II*, *49*, 1441–1457.

Lee, T. (2004), Decadal weakening of the shallow overturning ciruclation in the South Indian Ocean, *Geophys. Res. Lett.*, *31*, L18305, doi:10.1029/2004GL020884.

Lee, T., and M. J. McPhaden (2008), Decadal phase change in large-scale sea level and winds in the Indo-Pacific region at the end of the 20th century, *Geophys. Res. Lett.*, *35*, L01605, doi:10.1029/2007GL032419.

Maltrud, M. E., and J. L. McClean (2005), An eddy resolving global 1/10° ocean simulation, *Ocean Modell.*, *8*, 31–54, doi:10.1016/j.ocemod.203.12.001.

Marshall, J., A. Adcroft, C. Hill, L. Perelman, and C. Heisey (1997), A finite-volume, incompressible Navier Stokes model for studies of the ocean on parallel computers, *J. Geophys. Res.*, *102*(C3), 5753–5766.

McDonagh, E. L., H. L. Bryden, B. A. King, R. J. Sanders, S. A. Cunningham, and R. Marsh (2005), Decadal changes in the South Indian Ocean thermocline, *J. Clim.*, *18*, 1575–1590.

Menemenlis, D., I. Fukumori, and T. Lee (2005), Using Green's functions to calibrate an ocean general circulation model, *Mon. Weather Rev.*, *133*, 1224–1240.

Nauw, J. J., H. M. van Aken, J. R. E. Lutjeharms, and W. P. M. de Ruijter (2006), Intrathermocline eddies in the Southern Indian Ocean, *J. Geophys. Res.*, *111*, C03006, doi:10.1029/2005JC002917.

Nauw, J. J., H. M. van Aken, A. Webb, J. R. E. Lutjeharms, and W. P. M. de Ruijter (2008), Observations of the southern East Madagascar Current and Undercurrent System, *J. Geophys. Res.*, *113*, C08006, doi:10.1029/2007JC004639.

Palastanga, V., P. J. van Leeuwen, and W. P. M. de Ruijter (2006), A link between low frequency meso-scale eddy variability around Madagascar and the large-scale Indian Ocean variability, *J. Geophys. Res.*, *111*, C09029, doi:10.1029/2005JC003081.

Phillips, H. E., S. E. Wijffels, and M. Feng (2005), Interannual variability in the freshwater content of the Indonesian-Australian Basin, *Geophys. Res. Lett.*, *32*, L03603, doi:10.1029/2004GL021755.

Quartly, G. D., and M. A. Srokosz (2004), Eddies in the southern Mozambique Channel, *Deep Sea Res., Part II*, *51*, 69–83, doi:10.1016/j.dsr2.2003.03.001.

Ridderinkhof, H., and W. P. M. de Ruijter (2003), Moored current observations in the Mozambique Channel, *Deep Sea Res., Part II*, *50*, 1933–1955.

Schouten, M. W., W. P. M. de Ruijter, and P. J. van Leeuwen (2002), Upstream control of Agulhas Ring shedding, *J. Geophys. Res.*, *107*(C8), 3109, doi:10.1029/2001JC000804.

Schouten, M. W., W. P. M. de Ruijter, and H. Ridderinkhof (2005), A seasonal intrusion of subtropical water in the Mozambique Channel, *Geophys. Res. Lett.*, *32*, L18601, doi:10.1029/2005GL023131.

Song, Q., A. L. Gordon, and M. Visbeck (2004), Spreading of the Indonesian Throughflow in the Indian Ocean, *J. Phys. Oceanogr.*, *34*, 772–792.

Susanto, R. D., A. L. Gordon, and Q. Zheng (2001), Upwelling along the coasts of Java and Sumatra and its relation to ENSO, *Geophys. Res. Lett.*, *28*(8), 1599–1602.

Talley, L. D., and J. Sprintall (2005), Deep expression of the Indonesian Throughflow: Indonesian Intermediate Water in the South Equatorial Current, *J. Geophys. Res.*, *110*, C10009, doi:10.1029/2004JC002826.

Vranes, K., A. L. Gordon, and A. Ffield (2002), The heat transport of the Indonesian Throughflow and implications for the Indian Ocean heat budget, *Deep Sea Res., Part II*, *49*, 1391–1410.

Webb, D. J., B. A. de Cuevas, and A. C. Coward (1998), The first main run of the OCCAM global ocean model, *Tech. Rep. 34*, Southampton Oceanogr. Cent., Southampton, U. K.

Wyrtki, K. (1971), *Oceanographic Atlas of the International Indian Ocean Expedition*, Natl. Sci. Found., Washington, D. C.

Wyrtki, K. (1973), An equatorial jet in the Indian Ocean, *Science*, *181*, 262–264.

You, Y. (1997), Seasonal variations of thermocline circulation and ventilation in the Indan Ocean, *J. Geophys. Res.*, *102*(C5), 10,391–10,422.

You, Y., and M. Tomczak (1993), Thermocline circulation and ventilation in the Indian Ocean derived from water mass analysis, *Deep Sea Res., Part I*, *40*, 13–56.

————————————

W. P. M. de Ruijter, P. M. van der Werf, and P. J. van Leeuwen, Institute for Marine and Atmospheric Research Utrecht, Utrecht University, Princetonplein 5, NL-3584 CC Utrecht, Netherlands. (p.m.vanderwerf@uu.nl)

H. Ridderinkhof and M. W. Schouten, Department of Physical Oceanography, Royal Netherlands Institute for Sea Research, NL-1790 AB Texel, Netherlands.